Mitochondrial and nuclear DNA base excision repair are affected differently by caloric restriction

Jeff A. Stuart,*,[†] Bensu Karahalil,*,[‡] Barbara A. Hogue,* Nadja C. Souza-Pinto,* and Vilhelm A. Bohr*,[1]

*Laboratory of Molecular Gerontology, National Institute on Aging, National Institutes of Health, Baltimore, Maryland. [†]Current address: Department of Biology, Brock University, St. Catharines, Ontario, Canada. [‡]Current address: Gazi University, Faculty of Pharmacy, Toxicology Department, 06330, Ankara, Turkey

[1]Corresponding author: V. A. Bohr, 5600 Nathan Shock Dr., Box 1, Baltimore, MD 21224. E-mail: vbohr@nih.gov

ABSTRACT

Aging is strongly correlated with the accumulation of oxidative damage in DNA, particularly in mitochondria. Oxidative damage to both mitochondrial and nuclear DNA is repaired by the base excision repair (BER) pathway. The "mitochondrial theory of aging" suggests that aging results from declining mitochondrial function, due to high loads of damage and mutation in mitochondrial DNA (mtDNA). Restriction of caloric intake is the only intervention so far proven to slow the aging rate. However, the molecular mechanisms underlying such effects are still unclear. We used caloric-restricted (CR) mice to investigate whether lifespan extension is associated with changes in mitochondrial BER activities. Mice were divided into two groups, receiving 100% (PF) or 60% (CR) of normal caloric intake, a regime that extends mean lifespan by ~40% in CR mice. Mitochondria isolated from CR mice had slightly higher uracil (UDG) and oxoguanine DNA glycosylase (OGG1) activities but marginally lower abasic endonuclease and polymerase γ gap-filling activities, although these differences were tissue-specific. Uracil-initiated BER synthesis incorporation activities were significantly lower in brain and kidney from CR mice but marginally enhanced in liver. However, nuclear repair synthesis activities were increased by CR, indicating differential regulation of BER in the two compartments. The results indicate that a general up-regulation of mitochondrial BER does not occur in CR.

Key words: OGG1 • UDG • AP endonuclease • dietary restriction • aging • mitochondria

The basis of the modern free radical theory of aging was outlined by Harman in 1956 (1). Subsequently, abundant evidence has accumulated linking the oxidation of cellular macromolecules with aging and age-associated diseases. The rate of aging is under genetic control, and much progress has recently been made in understanding the genetic program underlying this process (2). Environmental factors also affect the rate of aging, perhaps most notably the restriction of caloric intake. Caloric restriction (CR) is a robust and apparently almost universal means of extending lifespan in organisms, from yeast to mammals. In addition to lifespan extension, CR decreases the occurrence of diseases associated with aging, including cancers (3) and neurodegenerative disorders (4).

Hart and Setlow (5) first described a strong correlation between the rate of unscheduled DNA repair and mammalian lifespan, suggesting a connection between DNA repair and lifespan. It has subsequently been shown that extension of lifespan within a given mammalian species, via CR, is also associated with an enhancement of unscheduled DNA repair (6). In both of these studies, unscheduled DNA repair was stimulated by UV irradiation of isolated cells, a treatment that is likely to promote primarily adducts that are repaired by the nucleotide excision repair pathway. However, aging is strongly correlated with the accumulation of oxidative damage, including oxidative DNA modifications, which are repaired primarily by the base excision repair (BER) pathway. BER is catalyzed in four consecutive steps by a DNA glycosylase, which removes the damaged base; an apurinic/apyrimidinic endonuclease, which processes the abasic site; a DNA polymerase, which inserts the new nucleotide(s); and DNA ligase, which rejoins the DNA strand. Cabelof et al. (7) recently reported that nuclear BER is enhanced in rats by CR, suggesting that BER plays a role in the lifespan extension associated with CR.

A wealth of evidence suggests that mitochondria are the most important cellular source of the reactive oxygen species (ROS) involved in macromolecular damage during the aging process (8). They are also critical targets of their action (9). Perhaps the most important target of ROS in mitochondria is mitochondrial DNA (mtDNA). Whereas oxidized protein and lipid can be replaced by de novo synthesis, oxidation of DNA can potentially lead to fixation of damage as mutation. The mutagenicity of the common oxidative mtDNA lesion 7,8-dihydroxyguanine (8-oxodG) has been demonstrated (10). The mitochondrial free radical hypothesis of aging proposes that the observed decline in mitochondrial function with aging results from mutated respiratory complex proteins, which cause enhanced superoxide production leading to further oxidation of macromolecules, including mtDNA (see 11 for review). Indeed, point mutations and deletions accumulate in the mtDNA of aging somatic cells (12). These are in some instances associated with the appearance of functional deficits, although the extent to which mitochondrial genomic instability plays a causative role remains to be determined.

Mitochondria efficiently remove oxidative DNA lesions, via the BER pathway. CR slows the age-associated accrual of oxidative damage in mitochondria (13) and lowers the levels of some oxidative mtDNA lesions (14, 15). Concomitant with decreased levels of oxidative damage in mtDNA, CR also appears to enhance mitochondrial genomic stability (16, 17). Thus, up-regulation of BER activity may be required to preserve both nuclear and mitochondrial genomic integrity in the longer-lived CR animals. Here we have tested this hypothesis by comparing mitochondrial and nuclear DNA repair activities in 16-month-old mice maintained on a 40% calorie-restricted diet for 14 months with pair-fed (PF; 100% caloric intake) controls. We measured the activities of individual enzymes that catalyze single steps in the BER pathway, such as the oxoguanine DNA glycosylase (OGG1), which recognizes and removes 8-oxodG from DNA; the uracil DNA glycosylase (UDG); endonuclease III homologue 1 (NTH1); AP endonuclease; and DNA polymerase γ. We also measured the total activity of the BER pathway by following uracil-initiated repair synthesis incorporation. These measurements of DNA repair activity provide insights into the extent of changes in BER efficiency in the maintenance of mitochondrial and nuclear genomic stability during caloric restriction.

MATERIALS AND METHODS

Animals

Six-week-old C57BL6 mice were obtained from Charles River Laboratories (Wilmington, MA), housed in the National Institute on Aging Gerontology Research Center animal colony, and fed a standard NIH-07 diet (Harlan-Teklad, Indianapolis). Food was provided ad libitum until 9 weeks of age. At that time, mice were randomly divided into two groups, one receiving 100% of the average ad libitum food consumption (PF group) and the other 60% (CR group). Water was available ad libitum. The animals were kept on a 12 h light:dark schedule. At ~14 months of age, mice were killed by cervical dislocation, and hearts, brains, livers and kidneys were removed, placed on ice, and used immediately for preparation of mitochondrial and nuclear extracts. All experiments were performed in accordance with the Guidelines for the Use and Care of Laboratory Animals (NIH publication 85-23).

Materials

All chemicals were ACS grade and purchased from Sigma (St. Louis, MO), with the following exceptions. Leupeptin and benzamide were from Roche (Indianapolis, IN). Isotopes were from NEN Life Science Products (Boston, MA), and G25 columns were from Amersham (Little Chalfont, UK). T4 polynucleotide kinase and T4 DNA ligase were from Stratagene (San Diego, CA). Tris-glycine gels for protein electrophoresis and PVDF membranes for Western blotting were from Invitrogen (Carlsbad, CA).

Oligonucleotides

Control and modified oligonucleotides were from Midland Certified Reagent Co. (Midland, TX), except 5-OH-deoxycytosine and 5-OH-deoxyuracil, which were kindly provided by Michelle Ham (Massachusetts Institute of Technology, Cambridge, MA). The sequences of all oligonucleotides used are presented in Table 1. For BER synthesis assays, an unlabeled uracil-containing double-stranded oligonucleotide was used. For incision assays, oligonucleotides containing either a defined lesion or an unmodified base (controls) were 5′-end labeled with T4 polynucleotide kinase and $[\gamma\text{-}^{32}P]ATP$. Reaction mixtures were centrifuged through Sephadex G-25 columns to remove unincorporated $[\gamma^{32}P]ATP$, then annealed to their complement, with the exception of uracil, which was used in single stranded form for incision assays.

Isolation of mitochondrial and nuclear fractions

Protocols for mitochondrial isolation were tissue specific. Liver and kidney mitochondria were prepared essentially as described in Croteau et al. (18). Briefly, tissues were minced, placed in 10 volumes of MSHE buffer (0.21 M mannitol; 70 mM sucrose; 10 mM HEPES; 1 mM EGTA; 2 mM EDTA; 0.15 mM spermine; 0.75 mM spermidine; 5 mM dithiothreitol; 2 µg/ml leupeptin; 2 µg/ml benzamide, pH 7.4) and homogenized with a Potter-Elvejhem homogenizer. Mitochondria isolated by differential centrifugation were further purified by Percoll gradient centrifugation (1:1 mixture of 2 × MSHE and Percoll (Amersham Biosciences, Uppsala, Sweden). The pellet (nuclear fraction) from the first low-speed centrifugation step was collected and frozen at −80°C

for preparation of nuclear extracts. The mitochondrial band from the Percoll gradient centrifugation step was washed twice in MSHE and frozen at −80°C for future use.

Heart and brain mitochondria were isolated essentially as described in Karahalil et al. (19). For heart mitochondria, hearts were placed in 5 ml of ice-cold MSHE and minced. Buffer was discarded and 5 ml of fresh MSHE added. Protease (0.5 mg; Nagarse, Sigma) was added, and hearts were homogenized gently and slowly for 8 min. The homogenate was centrifuged at 9500 g for 9 min, the pellet was resuspended in MSHE (without protease) and homogenized with another 10 strokes. This homogenate was centrifuged at 500 g for 12 min. The pellet (nuclear fraction) was stored at −80°C for future use. Mitochondria were isolated by centrifugation of the supernatant at 9500 g for 9 min, followed by a single wash in MSHE. For brain mitochondria isolation, brains were placed in MSHE and homogenized with 15 passes of a Potter-Elvejhem homogenizer. Homogenates were centrifuged at 1200 g for 12 min. The pellet (nuclear fraction) was stored at −80°C for future use. Mitochondria were sedimented by centrifugation at 10,500 g for 15 min, then resuspended in MSHE/3% Ficoll 400, gently layered onto an equal volume of 6% Ficoll 400, and centrifuged at 10,500 g for 25 min. The mitochondrial pellet was washed in MSHE, and digitonin was added to 1.5 mg/ml and incubated on ice for 15 min. This suspension was centrifuged at 10,500 g for 15 min and washed once in MSHE. The resultant mitochondrial fraction was stored at −80°C.

Western blots

Nuclear contamination of mitochondrial fractions was assessed by probing for the presence of the abundant nuclear protein Lamin B2 by Western blot. Mitochondrial or nuclear protein (60 µg) was diluted 1:1 in protein loading buffer (Invitrogen, Carlsbad, CA), supplemented with 50 mM 2-mercaptoethanol, sonicated, heated at 90°C for 10 min, centrifuged briefly, and then separated in an 8–16% Tris-glycine gel (130 V, 1.5 h). Proteins were transferred to PVDF membranes (250 mA, 2 h), blocked overnight at 4°C in phosphate buffered saline containing 0.1% Tween 20 and 5% milk protein. Membranes were probed with a 1:500 dilution of anti-Lamin B2 (Novocastra, Newcastle upon Tyne, UK). Equal protein loading and transfer was determined by amido black staining of membranes.

Preparation of mitochondrial extracts

Mitochondrial fractions were treated as described in Souza-Pinto et al. (20) before use in incision assays for measurements of DNA glycosylase or AP endonuclease activities. For measurements of BER synthesis, mitochondrial extracts were prepared as following: ~50 µl of mitochondrial suspension was made up to 250 µl in lysis buffer A (20 mM HEPES, pH 7.5; 1 mM EDTA; 5% glycerol; 0.5% Triton X-100; 300 mM KCl; 5 mM DTT; 1 µg/ml aprotonin; 1 µg/ml pepstatin A; 1 µg/ml chymostatin A; 2 µg/ml leupeptin; 2 µM benzamide; 1 mM PMSF; and 1 µM E-64). The mixture was incubated on ice for 30 min, with occasional vortexing, then centrifuged at 130,000 g for 1 h. The lysis buffer was exchanged for buffer B (as buffer A, but with 100 mM KCl, 25% glycerol, 0.015% Triton X-100) and concentrated to ~100 µl, using Microcon 30 (Millipore) microconcentrators. Mitochondrial extracts were stored at −80°C.

Preparation of nuclear extracts

Nuclear extracts were prepared from nuclear pellets isolated as described above. Pellets were thawed and centrifuged at 20,000 g for 20 min. Five volumes of lysis buffer A (as above) were added, and the suspension incubated on ice for 10 min, vortexed twice. The mixture was centrifuged at 130,000 g for 1 h. The supernatant was concentrated and exchanged for buffer B using Microcon 30. The nuclear extracts were stored at –80°C.

DNA glycosylase assays

Incision of uracil, 5-OH-uracil, or 5-OH-cytosine in 30-mer oligonucleotides (see Table 1) was measured essentially as described in Nyaga and Bohr (21). Reactions (20 μl) contained 70 mM HEPES (pH 7.5), 1 mM EDTA, 1 mM DTT, 75 mM NaCl, 0.5% BSA, 90 fmol of oligonucleotide, and 25 μg of nuclear or mitochondrial protein. Assays were incubated at 37°C for 1 h and terminated as described below. Incision of 8-oxodG from a 28-mer oligonucleotide was measured essentially as in (20). Reactions (20 μl) contained 40 mM HEPES (pH 7.6), 5 mM EDTA, 1 mM DTT, 75 mM KCl, 10% glycerol, 88.8 fmol of oligonucleotide, and 50 μg mitochondrial or nuclear protein. Reactions were incubated for 6 (mitochondria) or 2 h (nucleus) at 32°C then terminated by adding 5 μg of proteinase K (PNK) and 1 μl of 10% SDS and incubating at 55°C for 30 min. DNA was precipitated by addition of 1 μg glycogen, 4 μl of 11 M ammonium acetate, 60 μl of ethanol, and overnight incubation at –20°C. Samples were centrifuged, dried, suspended in 10 μl of formamide loading dye (80% formamide, 10 mM EDTA, 1 mg/ml xylene cyanol FF, and 1 mg/ml bromophenol blue) and loaded onto a 20% acrylamide and 7 M urea gel. Substrate and product DNA were resolved by electrophoresis at 15 W for 1 h 10 min. Gels were visualized by PhosphorImager and analyzed by using ImageQuant[TM] (Molecular Dynamics). Incision activity was determined as the intensity of product bands relative to the combined intensities of substrate and product bands.

AP endonuclease assays

AP endonuclease activity in mitochondria and in nuclear extracts was assayed in 50 mM HEPES (pH 7.5), 50 mM KCl, 100 μg/ml BSA, 10 mM $MgCl_2$, 10% glycerol, and 0.05% Triton X-100. Double-strand oligonucleotide substrate (1 pmol) containing a tetrahydrofuran (abasic site analog; Table 1), and 500 ng (mitochondria) or 50 ng (nuclear) extract were added to a final reaction volume of 10 μl. Reaction mixtures were incubated at 37°C for 10 min. The reactions were terminated by addition of 10 μl of formamide loading dye and incubation at 95°C for 10 min. Samples were loaded directly on gels and analyzed as above.

Base excision repair synthesis assays

Repair synthesis of a uracil containing duplex was measured in mitochondrial and nuclear extracts, essentially as described in Nyaga and Bohr (21). Reactions contained 40 mM HEPES, 0.1 mM EDTA, 5 mM $MgCl_2$, 0.2 mg/ml BSA, 50 mM KCl, 1 mM DTT, 40 mM phosphocreatine, 100 ug/ml phosphocreatine kinase, 2 mM ATP, 40 μM dNTPs, 4μCi ^{32}P-dCTP, 3% glycerol, and 120 ng double-strand oligonucleotide, in 20 ul. Nuclear or mitochondrial extract (40 μg) were added, and reaction mixtures were incubated at 37°C for 15, 30, or 60 min, followed by addition of 1 unit of T4 DNA ligase. Reactions were terminated and processed as

described above for DNA glycosylase assays. Substrate and product DNA were resolved by electrophoresis at 15 W for 1 h 10 min. Gels were visualized by PhosphorImager and analyzed by using ImageQuant^{TM} (Molecular Dynamics). Quantification of repair synthesis activity was performed by comparing the average relative intensities of the ^{32}P-dCTP-containing 30-mer in CR vs. PF extracts.

Polymerase γ assays

Polymerase γ gap-filling activity was measured by using essentially the same approach as for measurement of uracil-initiated repair synthesis outlined above, except a 39-mer oligonucleotide containing a single nucleotide gap was used (GAP; Table 1). In these assays 5 ug of brain or kidney mitochondrial extract was incubated with 1 pmol of GAP oligonucleotide in a final assay volume of 10 µl for 100 min at 37°C, followed by addition of 10 units T4 ligase and continued incubation for 20 min to ensure full product ligation.

RESULTS

Nuclear contamination of mitochondrial fractions was assessed using Western blot to probe for the highly abundant nuclear protein Lamin B2 (Fig. 1). Lamin B was detected in nuclear pellets, but no signal was present in mitochondrial fractions, which were thus free of nuclear contamination. Equal protein loading of nuclear and mitochondrial fractions was confirmed by amido black staining (not shown).

Effects of CR on mitochondrial BER pathway flux

The ability of mitochondria to remove DNA damage, to process and fill the resultant gap, and to religate the DNA strands (BER synthesis) was measured by monitoring the incorporation of ^{32}P-dCTP into a double-strand oligonucleotide containing a single uracil at a defined position (dsU; see Table 1). Following incubation of the oligonucleotide with the mitochondrial extracts, a saturating amount of T$_4$ DNA ligase was added to promote complete ligation of repaired but unligated DNA, thus allowing quantification of a single, 30-nucleotide, band. Fig. 2a shows a representative gel in which the repaired oligonucleotide has been resolved. BER synthesis activity was determined at three time points to ensure that repair capacity was not saturated under these experimental conditions (Fig. 2b, d, f). Incubation of the extracts with a control oligonucleotide (dsC; see Table 1) typically produced negligible synthesis incorporation. Where ^{32}P-dCTP incorporation into the control oligonucleotide was detected, it was subtracted as background from the dsU values (not shown). Statistical comparisons of the mean levels of product were made at 90 (liver, kidney) or 60 min (brain). The effect of CR on mitochondrial BER was found to be tissue-dependent. In liver, ~18% more repaired product was present at 90 min in CR mice, although this was not statistically significant (Fig. 2c). In contrast, the rate of dsU repair was significantly lower in kidney (Fig. 2e) and brain (Fig. 2g) mitochondria of CR mice. Both tissues had ~30% lower mitochondrial BER activities than in PF mice ($P \leq 0.06$). Thus, the effect of CR on mitochondrial BER activity was tissue-specific.

Activities of individual steps in the BER pathway were measured to determine the source(s) of differences in pathway flux. The first three steps in uracil-initiated BER synthesis are catalyzed by UDG, AP endonuclease, and polymerase γ. Mitochondrial UDG activity was measured using

the ssU (Table 1) oligonucleotide. Mitochondrial lysates used for these measurements have high AP endonuclease activities, which catalyze the cleavage of the abasic strand following UDG removal of uracil. A representative gel showing full-length ssU and the 11-nt product is presented in Fig. 3a. UDG activity was slightly enhanced in mitochondria from all tissues examined, although this was statistically significant only in kidney, where UDG activity was almost 40% greater in CR mice (Fig. 3b). AP endonuclease activity was measured by using a THF (abasic site analog) containing oligonucleotide (Table 1). The kinetics of AP endonuclease activity is particularly rapid under the conditions of the assay used here. Therefore, this activity was determined at different time points, from 3 to 10 min, to ensure that saturation of incision activity did not occur (data not shown). AP endonuclease activity was found to be approximately linear over this range, and statistical comparisons were made at 10 min (Fig. 3d). Mitochondrial AP endonuclease activities were marginally lower in all tissues of CR mice examined, except in brain, where an ~55% ($P<0.05$) decrease occurred. This tissue also had significantly lower mitochondrial uracil-initiated repair synthesis incorporation activity (Fig. 2f, g). Polymerase γ gap-filling activities were measured in brain and kidney mitochondrial extracts, in which uracil-initiated repair synthesis incorporation activities were reduced in CR mice. Polymerase γ activity in kidney mitochondria was 29% lower in CR mice relative to controls ($P = 0.07$; Fig. 3e). Brain polymerase γ activity was ~20% lower in CR mice ($P = 0.21$; Fig. 3f).

DNA glycosylases each recognize a defined subset of DNA lesions. We next measured the activities of OGG1 and NTH1 in mitochondria from CR and PF mice using oligonucleotides containing 8-oxodG and 5-OHdC/5-OHdU, respectively (Table 1), to determine whether repair of oxidative DNA damage is also modulated by CR. Incision of 8-oxodG was almost 20% greater in liver mitochondria of CR mice ($P<0.05$), but not different in brain or heart mitochondria (Fig. 4a). Incision of 5-OH uracil and 5-OH cytosine were marginally decreased in CR mouse kidney mitochondria (Fig. 4b, c), but only the 5-OH cytosine measurement was significantly different ($P<0.05$). No significant differences in NTH1 activities were found for other tissues.

Thus, CR induced tissue-specific changes in mitochondrial DNA repair activities. However, a general up-regulation of mitochondrial DNA repair was not observed.

Effects of CR on nuclear BER

BER synthesis activity was also measured in liver and kidney nuclear extracts from CR and PF mice. The appearance of the repaired oligonucleotide containing the ^{32}P-dCTP was measured following incubation for 45, 60, or 90 min. Fig. 5a shows a representative gel in which the repaired 30-mer has been resolved. Statistical comparisons were made between values measured at 90 min. A control oligonucleotide containing no uracil was also used to assess background levels of ^{32}P-dCTP incorporation (not shown). The effect of CR on nuclear BER synthesis activity differed from that found in mitochondria. An ~26% enhancement of BER synthesis activity was found in liver nuclear extracts of CR mice relative to PF (Fig. 5b), although this was not statistically significant. Kidney nuclear extracts of CR mice had ~42% greater BER activity than controls ($P<0.05$).

We measured UDG and AP endonuclease activities essentially as was done for mitochondrial fractions, but found no differences between CR mice and PF (Fig. 6). OGG1 and NTH 1 activities were also assessed and found to be unaffected by CR (Fig. 7).

DISCUSSION

Mutations in mtDNA accumulate with aging at a much faster rate than in nuclear DNA, and at faster rates in short-lived than in long-lived animals (22). They are thought to result primarily from high levels of oxidative damage, such as 8-oxodG, in the mitochondrial genome. Increased levels of 8-oxodG occur concomitantly with increased mutation load in aging (23) and in species with different maximum lifespans (24). One interpretation of these observations has been that mtDNA repair is less efficient in shorter-lived species, as are some forms of nuclear DNA repair (22). A corollary of this is that increasing mtDNA repair efficiency should increase lifespan by maintaining the integrity of the mitochondrial genome over a greater length of time. CR is a robust experimental manipulation that increases lifespan and resistance to oxidants and carcinogens (3) while decreasing the steady-state levels of mtDNA oxidative lesions (15, 25) and mtDNA mutation load (26). Here we have tested the hypothesis that CR initiates a program of enhanced mtDNA repair to reduce the accumulation of mutations and lengthen lifespan.

Our findings do not support the hypothesis of universally enhanced mtDNA repair in the CR model of lifespan extension, as no clear pattern of induction of mtDNA repair was observed. Although numerous tissue-specific increases in mtDNA repair activities were noted, the most significant effect of CR was a reduction of uracil-initiated BER activity in brain and kidney mitochondria. The absence of enhanced BER activity in mitochondria from these post-mitotic tissues was somewhat surprising, particularly as mtDNA oxidative damage (8-oxodG) and mutation load are both decreased in post-mitotic tissues by CR. However, the levels of mtDNA oxidative adducts, such as 8-oxodG, at a given time point represent an equilibrium between the opposing effects of de novo formation by oxidative attack and removal by BER. Lower steady-state levels of oxidative damage can therefore be achieved by lowering the rate of lesion formation. In mitochondria, a key source of oxidative stress is electron leakage to molecular oxygen during respiration, resulting in formation of superoxide anions on the matrix side of the inner membrane (27), apparently close to the site of mtDNA (28). The rate of superoxide generation by mitochondria in both liver and heart is decreased 45–50% by CR in mice (15, 25). The rate of formation of 8-oxodG in mtDNA is probably dependent on numerous factors, but all other parameters being equal, increased or decreased ROS production should affect a proportional increase or decrease, respectively, in lesion formation. Thus, a 45–50% reduction in rate of ROS formation, even combined with a 30% reduction in the rate of removal, will result in a lower steady-state level of lesions. This is in fact what is observed: mtDNA from post-mitotic tissues of CR mice have ~30% lower 8-oxodG levels than controls (15, 25, 29).

In contrast to kidney and brain, mitochondrial uracil-initiated repair synthesis incorporation activity in liver was maintained or perhaps slightly enhanced by CR. Similarly, OGG1 activity was increased by CR in liver mitochondria, but not in mitochondria from other tissues. These observations are consistent with data from studies of CR effects on liver mitochondria (23). Like heart mitochondria, liver mitochondria from CR mice produce 45–50% less ROS. However, whereas skeletal muscle and heart mtDNA 8-oxodG levels are ~30% lower in CR mice, levels of the lesion in liver mtDNA are 46% lower in CR. This finding suggests that the maintenance of

higher DNA repair capacity in livers of CR mice, combined with lower rates of lesion formation, affects greater reductions in the steady-state levels of lesion. Taken together with published data, our results allow us to conclude that the enhancement of mitochondrial genomic stability by CR involves an emphasis on decreasing ROS production at source, rather than reversing the effects of ROS-mediated mtDNA damage.

The lower BER activities of mitochondria from kidney and brain associated with CR suggest that mtDNA repair capacity in these tissues is regulated either by levels of oxidative lesions in mtDNA or directly by ROS. The agreement between the reductions in steady-state 8-oxodG levels and BER capacity is striking—30% reductions in both 8-oxodG levels in mtDNA in post-mitotic tissues (15) and BER capacity. Several recent publications suggest that mitochondrial BER activity is regulated by cellular oxidative stress. BER repair synthesis activity is up-regulated in brain following ischemia (30). Cytosolic AP endonuclease (APE1) translocates to mitochondria following H_2O_2 exposure (31). DNA polymerase γ activity in heart is increased fourfold by injection of the ROS-inducer adriamycin (32) Thus, it seems likely that mitochondrial BER is regulated, at least in part, by prevailing oxidative conditions in the cell or mitochondrial matrix.

Given that mtDNA glycosylase activities were not universally down-regulated by CR, how is the regulation of mitochondrial BER activity in CR achieved? Our data suggest that AP endonuclease and/or polymerase γ activities may be important determinants of overall BER capacity in mitochondria. AP endonuclease activities were lower in mitochondria from all tissues of CR mice, particularly brain. Translocation of APE1 from cytosol to mitochondria is regulated by oxidative stress (31), and the lower AP endonuclease activities in mitochondria from CR mice may therefore indicate reduced cellular oxidative stress in CR. However, neither the sensitivity of mitochondrial BER to AP endonuclease activity, nor the identity of the major mitochondrial AP endonuclease have been determined, so the significance of these observations with respect to BER activity is unclear.

Differences in polymerase γ activity closely paralleled changes in uracil-initiated BER activity in kidney and brain mitochondria, all of which were 20–30% lower in CR mice. These observations, and the particularly low deoxyribose phosphate lyase activity, an important step in the BER pathway, of polymerase γ (33) suggest that this enzyme may be particularly important in regulating overall mitochondrial BER activity in CR. Polymerase γ activity is apparently also highly responsive to cellular oxidative stress (32). Thus the reduced cellular oxidative stress of CR may down-regulate mitochondrial polymerase γ, and therefore BER, activities.

The reduced BER activities measured in kidney and brain mitochondria of CR mice were absent from liver mitochondria. This finding indicates a difference in the regulation of BER in mitotic vs. post-mitotic tissues in response to CR. A recent study from our laboratory (19) showed that mitochondrial DNA glycosylase activities are particularly high in tissues, like testes, with high mitotic potential. They are notably lower in post-mitotic tissues, even those such as heart, with high aerobic capacity. Amongst post-mitotic tissues (kidney, skeletal muscle, brain, and heart), OGG1 activity scaled to citrate synthase activity (an index of aerobic capacity) is remarkably similar. This indexed value is higher in liver and much higher in testes, both of which are mitotic tissues. Taken together with the present data, these results suggest that both oxidative stress and mitotic capacity are involved in the regulation of mitochondrial BER.

Effects of CR on nuclear BER differed markedly from mitochondria. Both kidney and liver uracil-initiated repair synthesis incorporation activities were higher in CR mice. This finding is in agreement with a previous report (7), which describes up-regulated nuclear BER in CR rats. The authors showed that BER synthesis and polymerase β activities both increase in tissues of CR rats, relative to controls. However, they did not measure other BER enzyme activities. We found no differences in the activities of DNA glycosylases (OGG1, UDG and NTH1) or AP endonuclease in nuclear extracts of CR mice. Taken together with the results of Cabelof et al. (7), this suggests polymerase β plays the central role in stimulating nuclear BER during CR. A recently published mathematical model of BER supports the idea that polymerase β exerts a high level of control over nuclear BER pathway activity (34).

In conclusion, the extension of lifespan and attenuation of mtDNA damage and mutation in post-mitotic cells achieved by CR is associated with alterations in mitochondrial BER but is not a universal up-regulation of repair activities. Indeed, in post-mitotic tissues such as kidney and brain, lower BER activities were found in CR mice. These lower BER activities may have been mediated by AP endonuclease and/or polymerase γ, in response to reduced intramitochondrial oxidative stress accompanying CR. In contrast, CR up-regulated nuclear BER activity. This finding was not associated with increased DNA glycosylase or AP endonuclease activities in the nucleus, consistent with a DNA polymerase β-mediated modulation of nuclear BER in CR.

ACKNOWLEDGMENTS

REFERENCES

1. Harman, D. (1956) Aging: a theory based on free radical and radiation chemistry. *J. Gerontol.* **11,** 298–300

2. Longo, V. D., and Finch, C. E. (2003) Evolutionary medicine: From dwarf model systems to healthy centenarians? *Science* **299,** 1342–1346

3. Hursting, S. D., Lavigne, J. A., Berrigan, D., Perkins, S. N., and Barrett, J. C. (2003) Calorie restriction, aging and cancer prevention: mechanisms of action and applicability to humans. *Annu. Rev. Med.* **54,** 131–152

4. Mattson, M. P., Chan, S. L., and Duan, W. (2002) Modification of brain aging and neurodegenerative disorders by genes, diet and behavior. *Physiol. Rev.* **82,** 637–672

5. Hart, R. W., and Setlow, R. B. (1974) Correlation between deoxyribonucleic acid excision-repair and life-span in a number of mammalian species. *Proc. Natl. Acad. Sci. USA* **71,** 2169–2173

6. Weraarchakul, N., Strong, R., Wood, W. G., and Richardson, A. (1989) The effect of aging and dietary restriction on DNA-repair. *Exp. Cell Res.* **181,** 197–204

7. Cabelof, D. C., Yanamadala, S., Raffoul, J. J., Guo, Z. M., Soofi, A., and Heydari, A. R. (2003) Caloric restriction promotes genomic stability by induction of base excision, repair and reversal of its age-related decline. *DNA Repair (Amst.)* **2,** 295–307

8. Harman, D. (1994) Aging – prospects for further increases in the functional lifespan. *Age (Omaha)* **17,** 119–146

9. Golden, T. R., and Melov, S. (2001) Mitochondrial DNA mutations, oxidative stress, and aging. *Mech. Ageing Dev.* **122,** 1577–1589

10. Pinz, K. G., Shibutani, S., and Bogenhagen, D. F. (1995) Action of mitochondrial DNA polymerase γ at sites of base loss or oxidative damage. *J. Biol. Chem.* **270,** 9202–9206

11. Lenaz, G. (1998) Role of mitochondria in oxidative stress and ageing. *Biochim. Biophys. Acta* **1366,** 53–67

12. Melov, S., Coskun, P. E., and Wallace, D. C. (1999) Mouse models of mitochondrial disease, oxidative stress, and senescence. *Mut. Res.* **434,** 233–242

13. Lass, A., Sohal, B. H., Weindruch, R., Forster, M. J., and Sohal, R. S. (1998) Caloric restriction prevents age-associated accrual of oxidative damage to mouse skeletal muscle mitochondria. *Free Rad. Biol. Med.* **25,** 1089–1097

14. Chung, M. H., Kasai, H., Nishimura, S., and Yu, B. P. (1992) Protection of DNA damage by dietary restriction. *Free Rad. Biol. Med.* **12,** 523–525

15. Gredilla, R., Sanz, A., Lopez-Torres, M., and Barja, G. (2001) Caloric restriction decreases mitochondrial free radical generation at complex I and lowers oxidative damage to mitochondrial DNA in the rat heart. *FASEB J.* **15,** 1589–1591

16. Lee, C. M., Weindruch, R., and Aiken, J. M. (1997) Age-associated alterations of the mitochondrial genome. *Free Rad. Biol. Med.* **22,** 1259–1269

17. Melov, S., Minerfeld, D., Esposito, L., and Wallace, D. C. (1997) Multi-organ characterization of mitochondrial genomic rearrangements in *ad libitum* and caloric restricted mice show striking somatic mitochondrial DNA rearrangements with age. *Nucleic Acids Res.* **25,** 974–982

18. Croteau, D.L., Rhys, C.M.J., Hudson, E.K., Dianov, G.L., Hansford, R.G. and Bohr, V.A. (1997) An oxidative damage-specific endonuclease from rat liver mitochondria. *J. Biol. Chem.* **272**, 27338–27344

19. Karahalil, B., Hogue, B. A., Souza-Pinto, N. C., and Bohr, V. A. (2002) Base excision repair capacity in mitochondria and nuclei: tissue-specific variations. *FASEB J.* **16,** 1895–1902

20. Souza-Pinto, N. C., Hogue, B. A., and Bohr, V. A. (2001) DNA repair and aging in mouse liver: 8-oxodG glycosylase activity increase in mitochondrial but not in nuclear extracts. *Free Rad. Biol. Med.* **30,** 916–923

21. Nyaga, S.G., and Bohr, V.A. (2002) Characterization of specialized mtDNA glycosylases. In *Mitochondrial DNA: Methods and Protocols* (Copeland, W.C., ed.) Humana Press, Totowa, NJ; pp. 227–244

22. Cortopassi, G. A., and Wang, E. (1996) There is substantial agreement among interspecies estimates of DNA repair activity. *Mech. Ageing Dev.* **91,** 211–218

23. Hudson, E. K., Hogue, B. A., Souza-Pinto, N. C., Croteau, D. L., Anson, R. M., Bohr, V. A., and Hansford, R. G. (1998) Age-associated change in mitochondrial DNA damage. *Free Rad. Res.* **29,** 573–579

24. Barja, G., and Herrero, A. (2000) Oxidative damage to mitochondrial DNA is inversely related to maximum life span in the heart and brain of mammals. *FASEB J.* **14,** 312–318

25. Lopez-Torres, M., Gredilla, R., Sanz, A., and Barja, G. (2002) Influence of aging and long-term caloric restriction on oxygen radical generation and oxidative DNA damage in rat liver mitochondria. *Free Rad. Biol. Med.* **32,** 882–889

26. Kang, C. M., Kristal, B. S., and Yu, B. P. (1998) Age-related mitochondrial DNA deletions: effect of dietary restriction. *Free Rad. Biol. Med.* **24,** 148–154

27. St. Pierre, J., Buckingham, J. A., Roebuck, S. J., and Brand, M. D. (2002) Topology of superoxide production from different sites in the mitochondrial electron transport chain. *J. Biol. Chem.* **277,** 44784–44790

28. Albring, M., Griffith, J., and Attardi, G. (1977) Association of a protein structure of probable membrane derivation with HeLa cell mitochondrial DNA near its origin of replication. *Proc. Natl. Acad. Sci. USA* **74,** 1348–1352

29. Drew, B., Phaneuf, S., Dirks, A., Selman, C., Gredilla, R., Lezza, A., Barja, G., and Leeuwenburgh, C. (2003) Effects of aging and caloric restriction on mitochondrial energy production in gastrocnemius muscle and heart. *Am. J. Physiol.* **284,** R474–R480

30. Chen, D. X., Minami, M., Henshall, D. C., Meller, R., Kisby, G., and Simon, R. P. (2003) Upregulation of mitochondrial base-excision repair capability within rat brain after brief ischemia. *J. Cereb. Blood Flow Metab.* **23,** 88–98

31. Frossi, B., Tell, G., Spessotto, P., Colombatti, A., Vitale, G., and Pucillo, C. (2002) H_2O_2 induces tranlocation of APE/Ref-1 to mitochondria in the Raji B-cell line. *J. Cell. Physiol.* **193,** 180–186

32. Ogihara, M., Tanno, M., Izumiyama, N., Nakamura, H., and Taguchi, T. (2002) Increase in DNA polymerase γ in the hearts of adriamycin-administered rats. *Exp. Mol. Pathol.* **73,** 234–241

33. Longley, M. J., Prasad, R., Srivastava, D. K., Wilson, S. H., and Copeland, W. C. (1998) Identification of 5′deoxyribose phosphate lyase activity in human DNA polymerase γ and its

role in mitochondrial base excision repair in vitro. *Proc. Natl. Acad. Sci. USA* **95,** 12244–12248

34. Sokhansanj, B. A., Rodrigue, G. R., Fitch, J. P., and Wilson, D. M. (2002) A quantitative model of human DNA base excision repair. I: mechanistic insights. *Nucleic Acids Res.* **30,** 1817–1825

Table 1

Oligonucleotide substrates used.

Name	Sequence
dsC	5'-ATA TAC CGC GGC CGG CCG ATC AAG CTT ATT-3'
	3'-TAT ATG GCG CCG GCC GGC TAG TTC GAA TAA-5'
ssC	5'-ATA TAC CGC GGC CGG CCG ATC AAG CTT ATT-3'
dsU	5'-ATA TAC CGC GG(U) CGG CCG ATC AAG CTT ATT-3'
	3'-TAT ATG GCG CC(G) GCC GGC TAG TTC GAA TAA-5'
ssU	5'-ATA TAC CGC GG(U) CGG CCG ATC AAG CTT ATT-3'
GAP	5'-CGG ATC TGC AGC TGA TGC GC-OH P–GTA CGG ATC CCC GGG TAC-3'
	3'-GCC TAG ACG TCG ACT ACG CGG CAT GCC TAG GGG CCC ATG-5'
OG	5'-GAA CGA CTG T(OG)A CTT GAC TGC TAC TGA T-3'
	3'-CTT GCT GAC A (C)T GAA CTG ACG ATG ACT A-5'
OHC	5'-ATA TAC CGC GG(OHC) CGG CCG ATC AAG CTT ATT-3'
	3'-TAT ATG GCG CC (G) GCC GGC TAG TTC GAA TAA-5'
OHU	5'-ATA TAC CGC GG(OHU) CGG CCG ATC AAG CTT ATT-3'
	3'-TAT ATG GCG CC (G) GCC GGC TAG TTC GAA TAA-5'
THF	5'-AAT TCA CCG GTA CG(F) TGA ATT CG-3'
	3'-TTA AGT GGC CAT GG(C) TCT TAA GC-5'

The important features are underlined: ds = double stranded; ss = single stranded; U = deoxy-uracil; OG = 8-oxodG; OHC = 5-OHdC; OHU = 5-OHdU; THF = tetrahydrofuran.
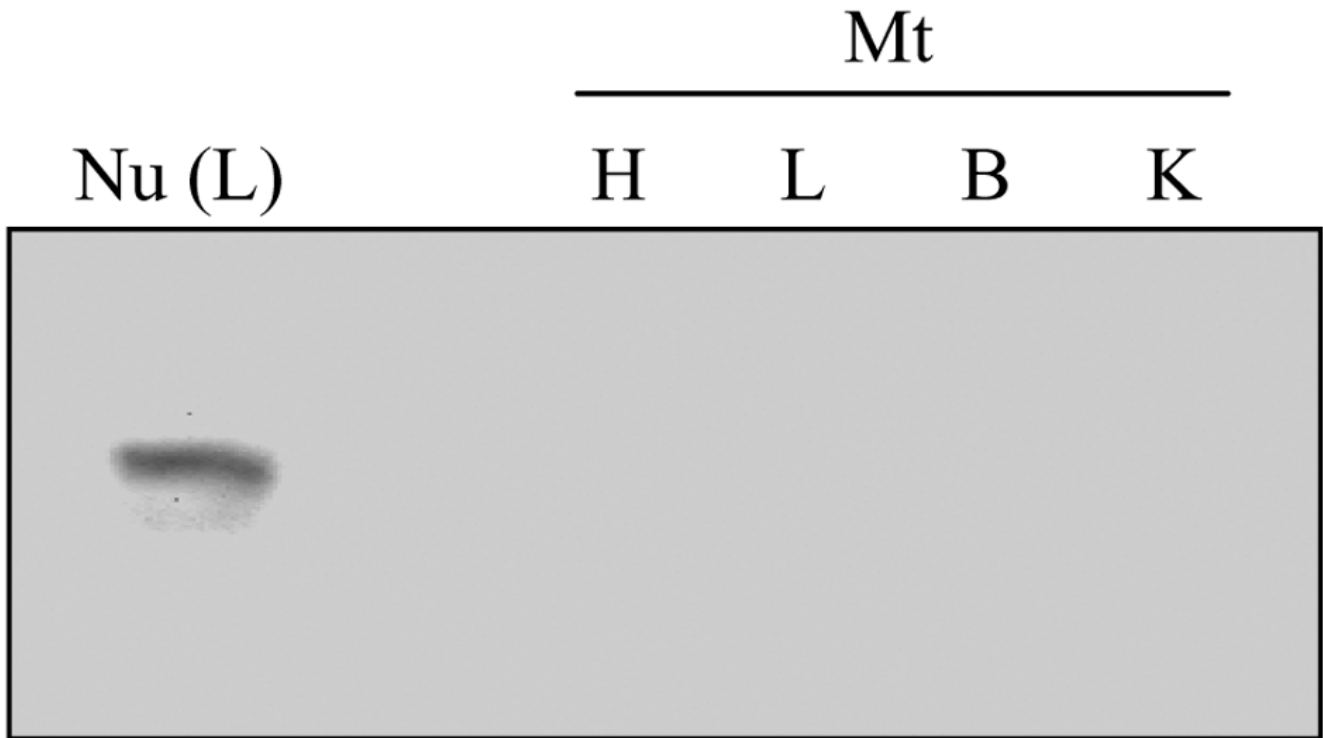
Fig. 1

Figure 1. Western blot analysis of Lamin B2 in nuclear and mitochondrial fractions isolated from mouse tissues.
Samples of 30 μg of liver nuclear or heart, liver, brain, or kidney mitochondrial extracts were loaded and resolved as described.
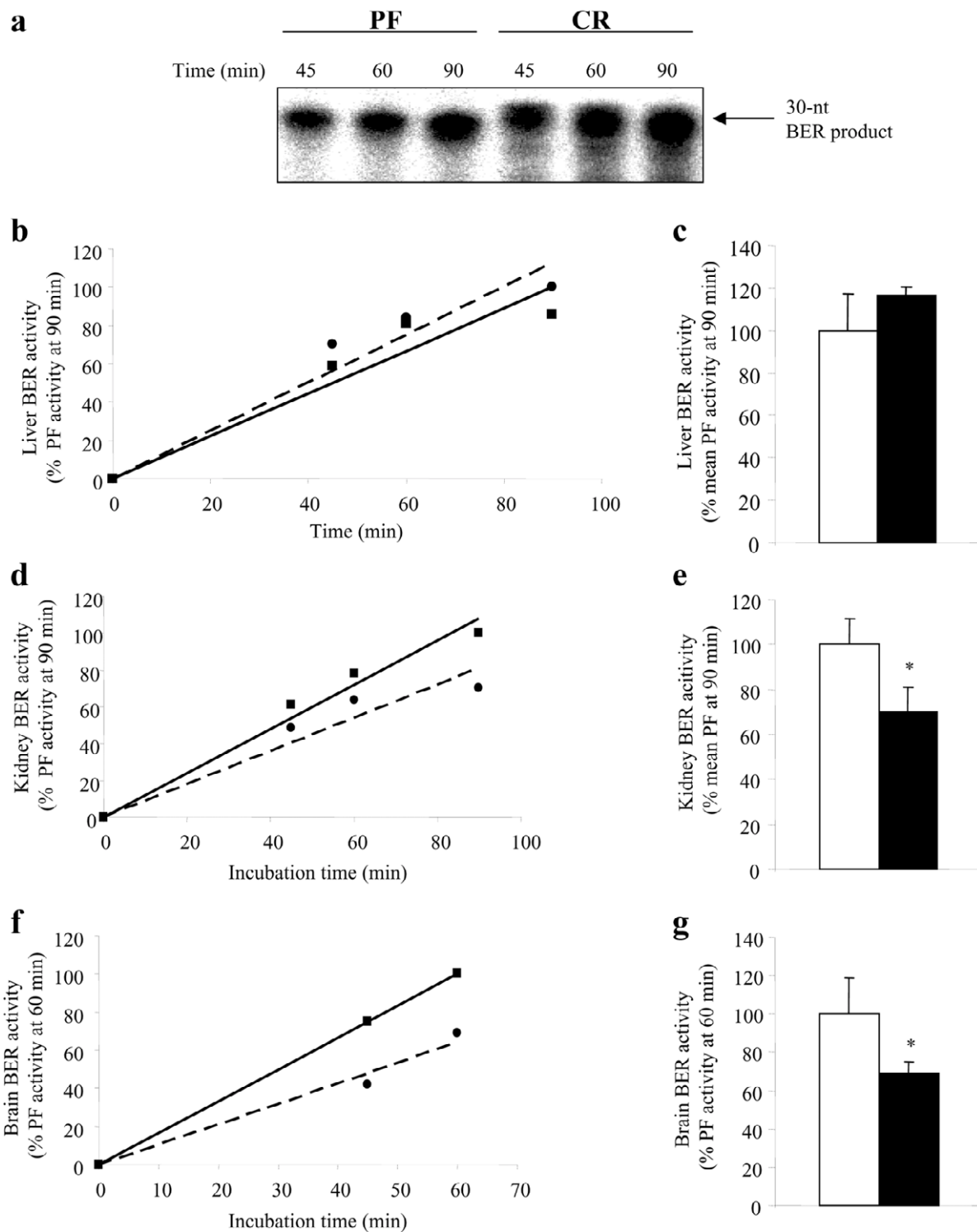
Fig. 2

Figure 2. BER synthesis in liver (*a–c*), kidney (*d*, *e*), and brain (*f*, *g*) mitochondrial extracts. *a*) A representative gel showing the product of uracil-initiated repair synthesis incorporation following incubation of dsU oligonucleotide with CR and PF liver mitochondrial extracts for 45, 60, or 90 min; (*b*) kinetics of dsU repair in liver mitochondria. Solid line = PF; broken line = CR.; (*c*) relative repair activity at 90 min. Repair activity was quantified as ^{32}P-dCTP signal strength, relative to PF = 100%. *d*) Kinetics of dsU repair in kidney mitochondria; (*e*) relative repair activity at 90 min. *f*) Kinetics of dsU repair in brain mitochondria; (*g*) relative repair activity at 60 min. For all graphs: squares = PF, circles = CR, open bars = PF, filled bars = CR. Values presented are means ± SE of duplicate measurements from four to five animals for each experimental group (error bars omitted from line graphs for clarity). * Denotes statistically significant difference [$P<0.05$ (brain); $P<0.065$ (kidney)].
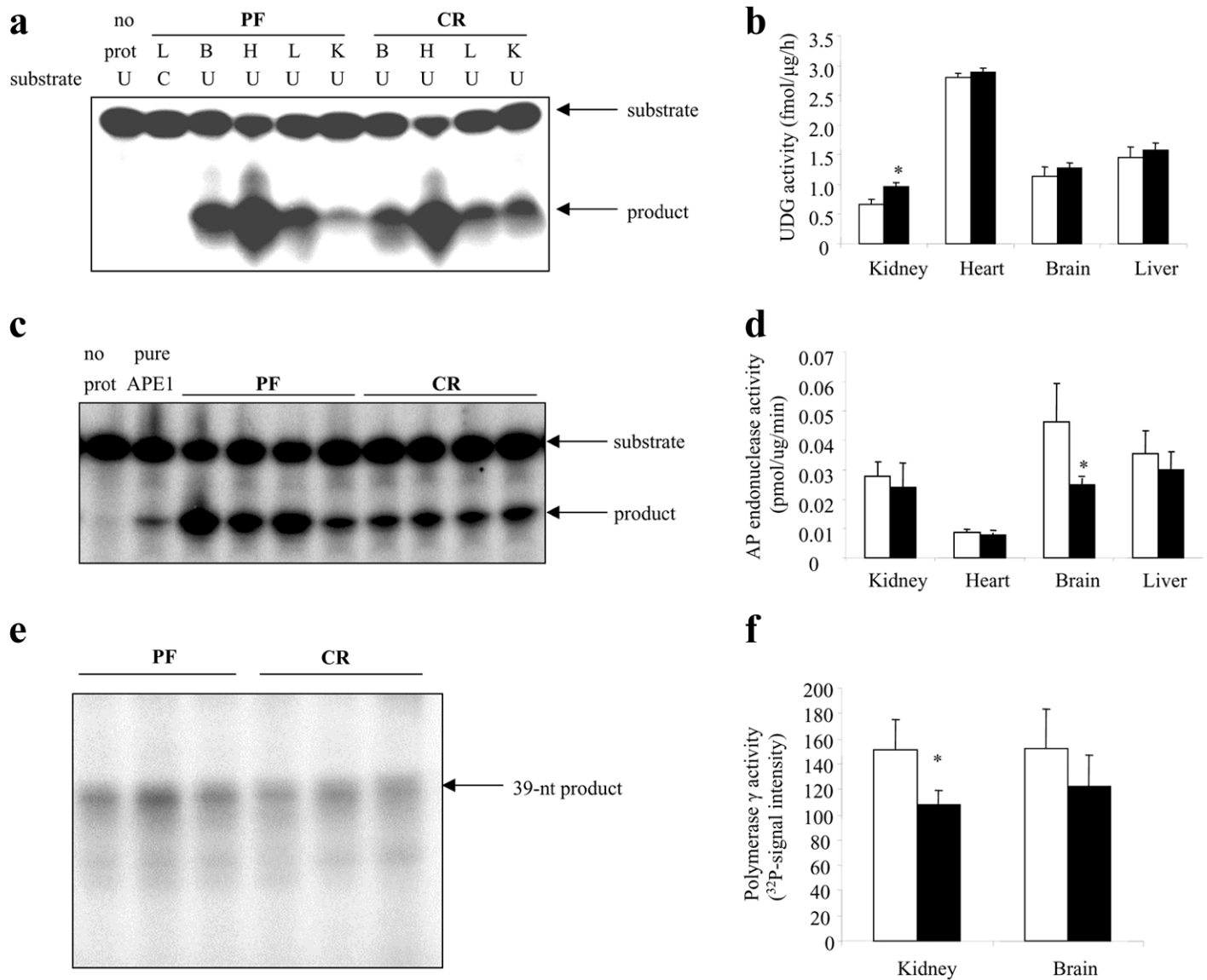
Fig. 3

Figure 3. DNA glycosylase, AP endonuclease and polymerase γ activities in mitochondria from CR and PF mice.
a) UNG activity: representative gel showing incision of a U-containing substrate by mitochondrial extracts. U = ssU oligonucleotide (substrate; see Table 1) ; C = ssC oligonucleotide; L = liver; B = brain; H = heart; K = kidney. *b*) UNG activity in CR and PF mice; (*c*) AP endonuclease activity: representative gel showing the incision of a THF-containing substrate. *d*) AP endonuclease activity in CR and PF mice; (*e*) polymerase γ gap-filling activity: representative gel showing the 39 nt product following incorporation of ^{32}P-dCTP into an oligonucleotide containing a 1 nt gap by kidney mitochondrial extracts from PF and CR mice; (*f*) mean gap-filling activities in kidney and brain mitochondria. *Denotes *P*=0.07 for comparison of PF and CR kidney.
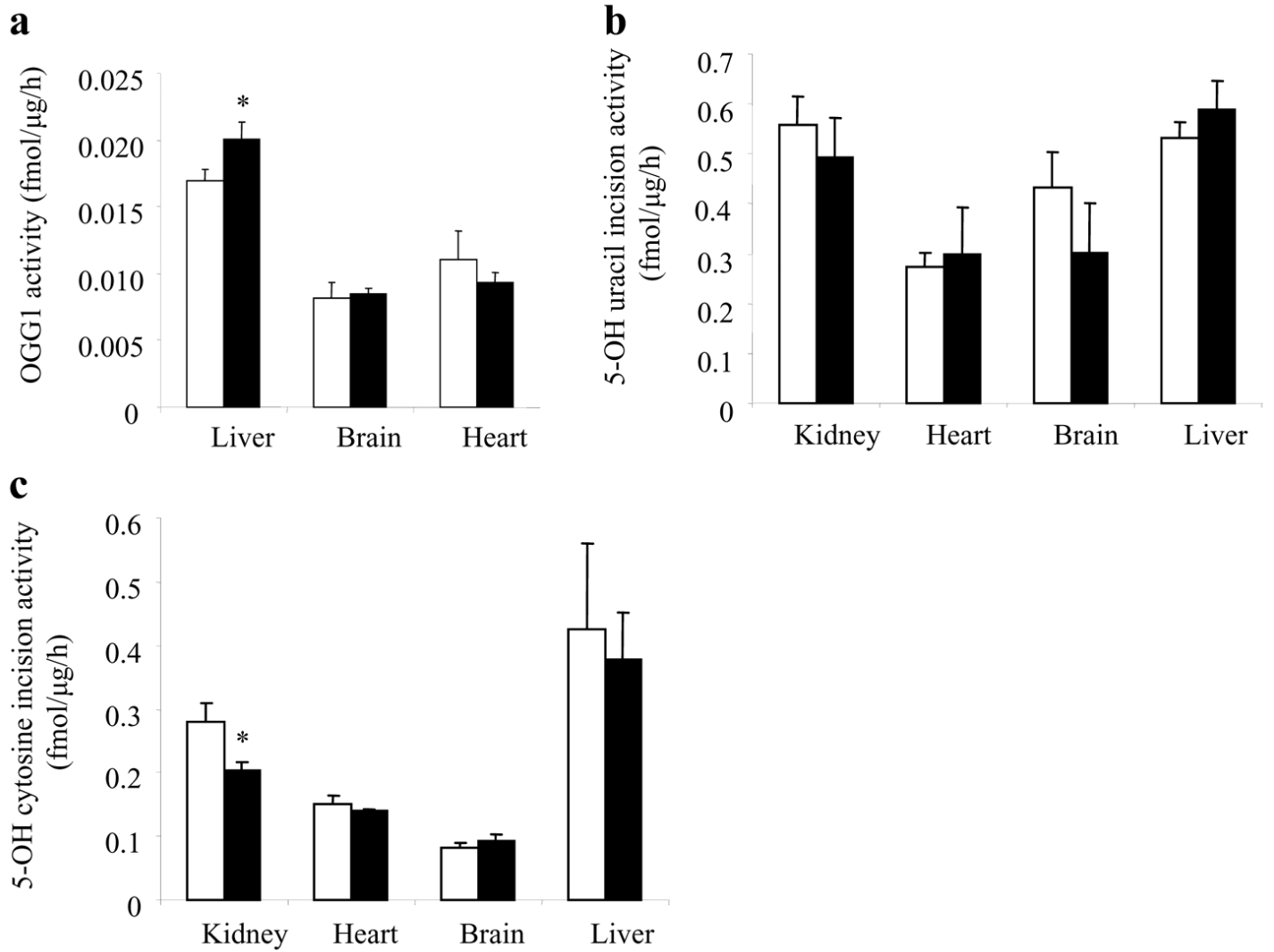
Fig. 4

Figure 4. *a*) OGG1 activity in CR and PF mouse mitochondria. *b*) OHU incision activity; (*c*) OHC incision activity. In all graphs, open bars = PF; filled bars = CR. Values are mean ± SEM (*n* = 5–6). *Significantly different from control mice (*P*<0.05).
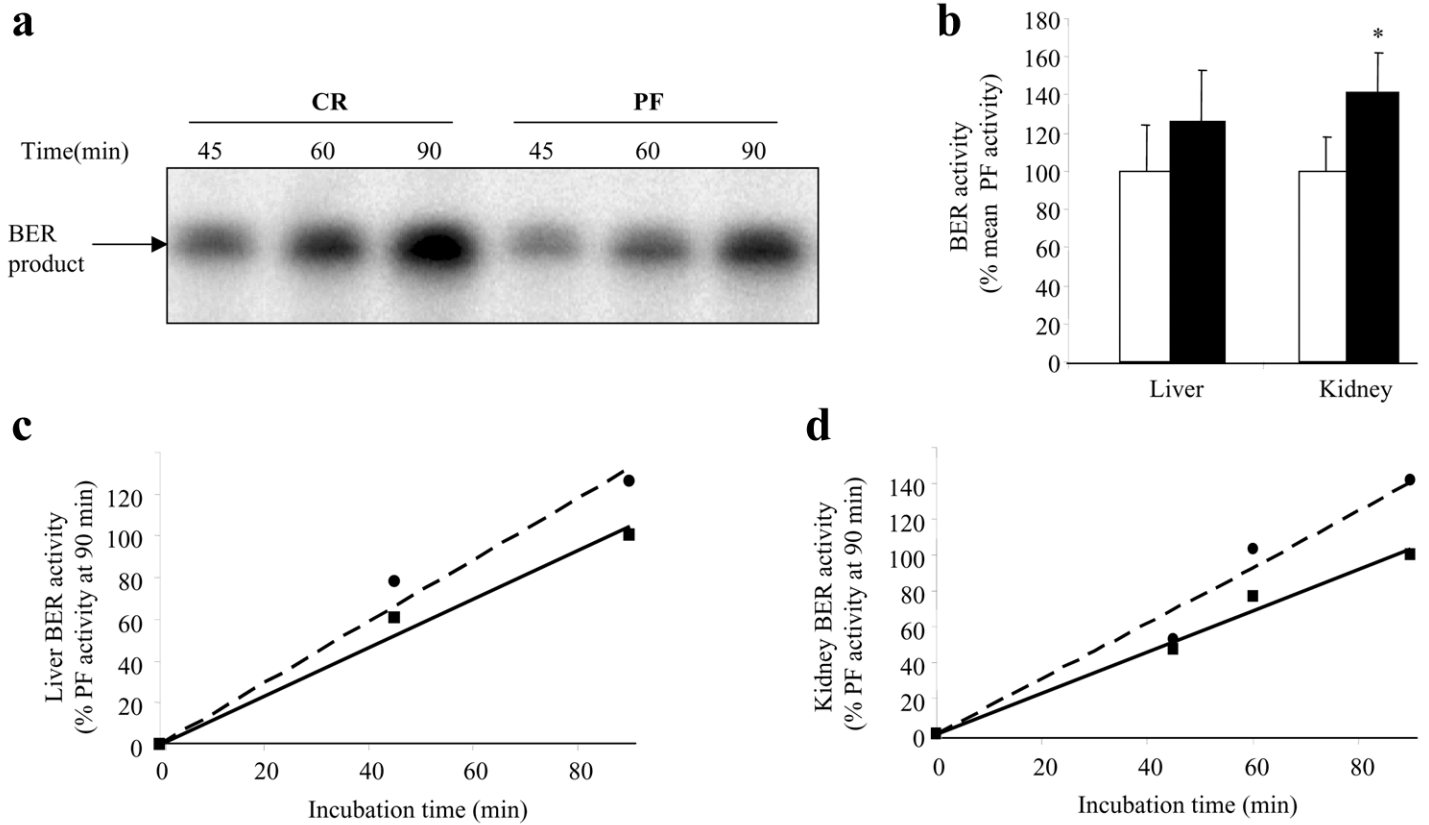
Fig. 5

a

b

c

d

Figure 5. BER synthesis in liver and kidney nuclear extracts. *a*) Representative gel showing BER product following incubation of dsU oligonucleotide with kidney nuclear extracts of CR and PF mice for 45, 60, or 90 min. *b*) Relative repair activity following 90 min incubation with liver and kidney nuclear extracts. Values are means ± SEM of duplicate or triplicate measurements on four to five independent samples. Open bars = PF mice, closed bars = CR mice. *Significantly different from control, *P*<0.05. *c*) Kinetics of BER synthesis in liver nuclear extracts. *d*) Kinetics of BER synthesis in kidney nuclear extracts. Squares = PF, circles = CR. Values in (*c*) and (*d*) are means of duplicate measurements from four to five individuals/experimental group. Error bars omitted for clarity.
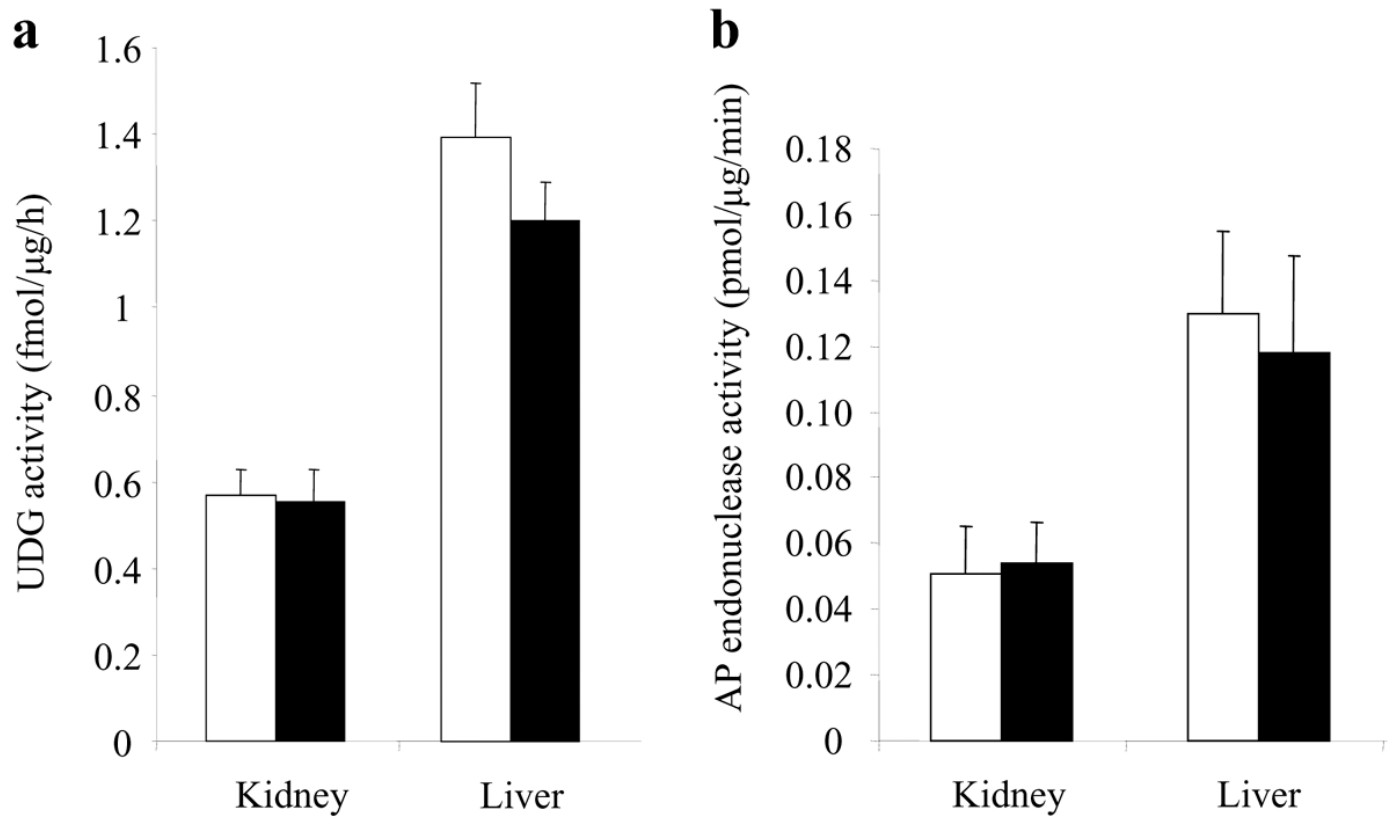
Fig. 6

Figure 6. UDG and AP endonuclease activities in nuclear extracts from CR and PF mice. *a*) Mean UDG activities; (*b*) Mean APE activities. Values are mean ± SEM (*n*=4–5).
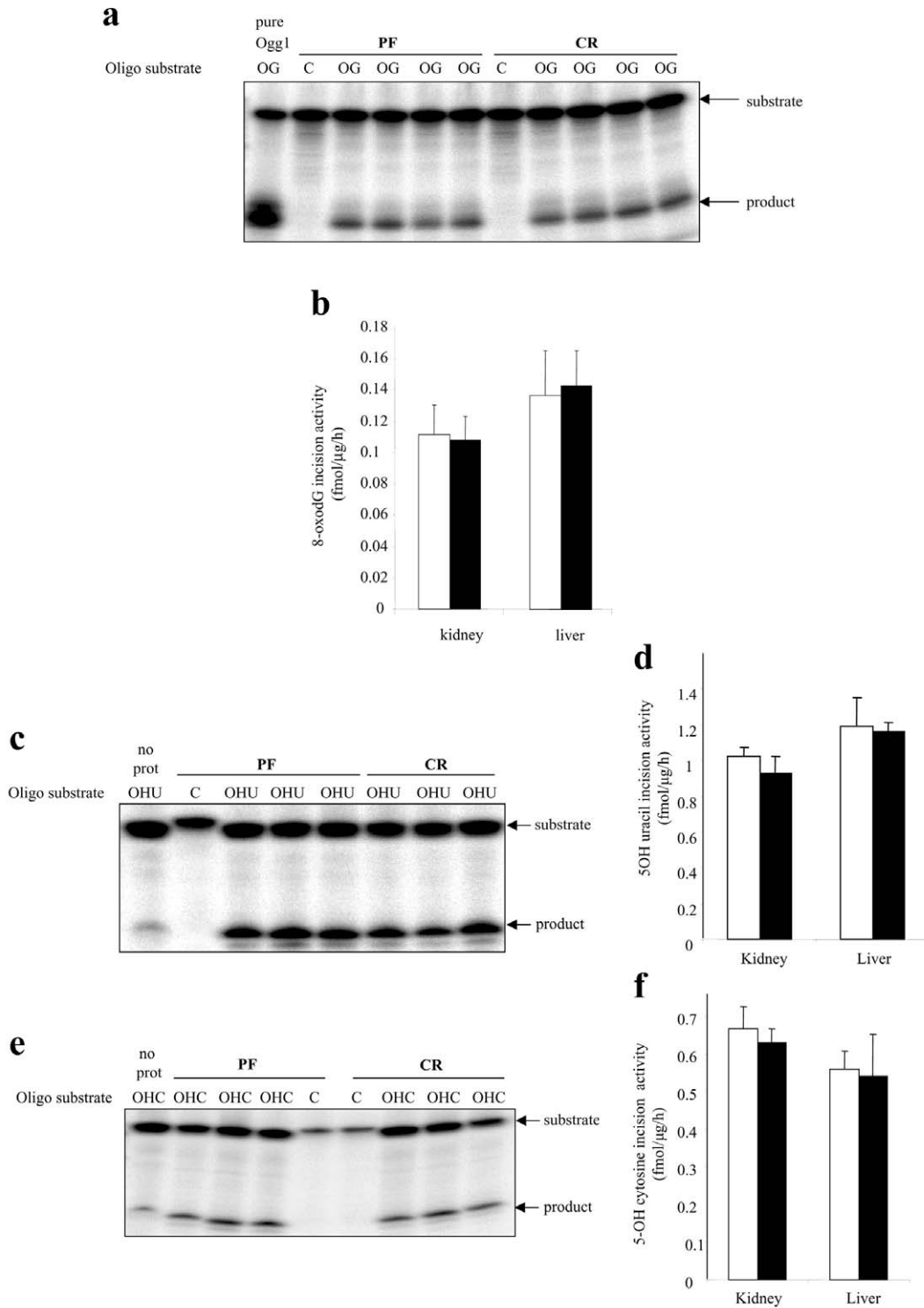
Fig. 7

Figure 7. OGG1 and NTH1 activities in nuclear extracts from CR and PF mice. *a*) Representative gel showing incision of an 8-oxodG substrate following incubation with kidney nuclear extracts. *b*) OGG1 activity in kidney and liver nuclear extracts. *c*) Representative gel showing incision of an OHU-containing oligonucleotide by liver nuclear extracts. *d*) OHU incision activity in kidney and liver nuclear extracts from CR and PF mice. *e*) Representative gel showing OHC incision by liver nuclear extracts. *f*) OHC incision activity in kidney and liver nuclear extracts. All values are mean ± SEM (*n* = 4–5). Open bars = PF; filled bars = CR.